Journal of Solid Mechanics Vol. 4, No. 2 (2012) pp. 209-225

Propagation of Waves at an Interface of Heat Conducting Elastic Solid and Micropolar Fluid Media

R. Kumar[1], M. Kaur[2,*], S.C. Rajvanshi[3]

[1]*Department of Mathematics, Kurukshetra University, Kurukshetra 136119, India*
[2]*Department of Applied Sciences, Guru Nanak Dev Engineering College, Ludhiana, Punjab 141008, India*
[3]*Department of Applied Sciences, Gurukul Vidyapeeth, Institute of Engineering and Technology, Banur, Sector 7, District Patiala, Punjab 140601, India*

Received 5 June 2012; accepted 5 July 2012

ABSTRACT

The present investigation is concerned with the reflection and transmission coefficients of plane waves at the interface of generalized thermoelastic solid half space and heat conducting micropolar fluid half- space. The amplitude ratios of various reflected and transmitted waves with various angle of incidence have been computed numerically and depicted graphically. Micropolarity and thermal relaxation effects are shown on the amplitude ratios for specific model. Some special and particular cases are also deduced from the present investigation.

Keywords: Elastic solid; Micropolar fluid; Thermoelastic; Reflection coefficient; Transmission coefficient; Angle of incidence

1 INTRODUCTION

THE theory of microfluids was introduced by Eringen [1]. A microfluid in addition to its classical translatory degrees of freedom represented by velocity field, possesses three gyration vector fields. As a subclass of these fluids, Eringen introduced the micropolar fluids [2] in which the local fluid elements were allowed to undergo only rigid rotations without stretch. Micropolar fluids can support couple stress, the body couples, asymmetric stress tensor and possesses a rotational field, which is independent of the velocity of fluid. A large class of fluids such as anisotropic fluids, liquid crystals with rigid molecules, magnetic fluids, cloud with dust, muddy fluids, biologicaltropic fluids, dirty fluids (dusty air, snow) over airfoil can be modeled more realistically as micropolar fluids. Various authors notably Ariman et.al. [3- 4], Riha [5], Eringen and Kafadar [6], Brulin [7], Gorla [8], Eringen [9], Aydemir and Venart [10], Hsia and Cheng [11], Hsia et al. [12] investigated different types of problem in micropolar fluid and heat conducting micropolar fluid.The theory of thermoelasticity deals with the effect of mechanical and thermal disturbances on an elastic body. The theory of uncoupled thermoelasticity consists of the heat equation, which is independent of mechanical effects and the equation of motion contains the temperature as a known function. Biot [13] formulated the theory of coupled thermoelasticity to eliminate the paradox inherent in the classical uncoupled theory that elastic changes have no effect on the temperature. The heat equations for both theories are of parabolic type predicting infinite speed of propagation for heat waves contrary to physical observations.

To overcome this drawback, two generalizations of coupled theory were introduced. The first is due to Lord and

* Corresponding author.
E-mail address: mandeep1125@yahoo.com (M. Kaur).

Shulman [14], who obtained a wave-type heat equation by postulating a new law of heat conduction to replace the classical Fourier's law.

The second generalization to the coupled theory of elasticity is known as the theory of thermoelasticity with two relaxation times or the theory of temperature-rate dependent thermoelasticity is given by Green and Lindsay [15]. A comprehensive review on thermoelasticity is available in the standard text e.g Dhaliwal and Singh [16] and Ignaczak and Starzewski [17] .

Various authors investigated the problems of reflection and transmission of plane waves at an interface of micropolar/micropolar elastic half- spaces. Tomar and Gogna [18-20], Kumar et al. [21-22], Singh and Tomar [23] have discussed the longitudinal waves at an interface of micropolar fluid/micropolar solid half- spaces. Inspite of these no work has been done at the interface of heat conducting elastic and micropolar fluid media.

In this paper, we study the problem of reflection of plane waves at an interface of generalized thermoelastic solid half-space and heat conducting micropolar fluid half-space. Micropolarity and thermal relaxation effects on the amplitude ratios for incidence of various plane waves that is Longitudinal wave (P-wave), Thermal wave (T-wave), Transverse wave (SV-wave) are computed numerically and illustrated graphically.

The exact nature of the earth is not known. One has to take different appropriate theoretical model to investigate the wave propagation problems. The study is motivated by the need for a better understanding of the role of interface on the propagation of plane waves between generalized thermoelastic solid half-space and heat conducting micropolar fluid half-space. All most all the oil companies rely on the sesmic interpretation for selecting the sites for exploratory oil wells. Seismic wavemethods also have higher accuracy, high resolution and are more economical as compared to drilling which is costly and time consuming. The model considered shows the kinds of waves travel through the medium which provides lot of information about the interior of earth. At the interface of these two media new types of waves encountered in micropolar fluid media which are not investigated thouroughly. Although it is a theoretical model but it has a great application in science, engineering and geophysics.

2 BASIC EQUATIONS

Following Lord and Shulman [14] and Green and Lindsay [15], the field equations for an isotropic and homogeneous elastic medium in the context of generalized theory of thermoelasticity, without body forces and heat sources, are given by:

$$(\lambda+2\mu)\nabla\left(\nabla.\vec{u}\right)-\mu(\nabla\times(\nabla\times\vec{u}))-\nu\left(1+\tau_1\frac{\partial}{\partial t}\right)\nabla T=\rho\frac{\partial^2\vec{u}}{\partial t^2}, \tag{1}$$

$$K^*\nabla T=\rho c^*\left(\frac{\partial T}{\partial t}+\tau_0\frac{\partial^2 T}{\partial t^2}\right)+\nu T_0\left(\frac{\partial}{\partial t}+\eta_0\tau_0\frac{\partial^2}{\partial t^2}\right)\left(\nabla.\vec{u}\right), \tag{2}$$

and the constitutive relations are

$$t_{ij}=\lambda u_{r,r}\delta_{ij}+\mu\left(u_{i,j}+u_{j,i}\right)-\nu\left(T+\tau_1\frac{\partial T}{\partial t}\right)\delta_{ij}\ , \qquad i,j,r=\ 1,2,3 \tag{3}$$

where symbols have their symbolic meaning. For Lord Shulman (L-S) theory $\eta_0=1$, $\tau_1=0$ and for Green-Lindsay (G-L) theory $\eta_0=0$, $\tau_1>0$. The thermal relaxation time τ_0 and τ_1 satisfy the inequalities $\tau_0\geq\tau_1\geq 0$ for G-L theory only.

Following Ciarletta [24], the field equations and the constitutive relations for heat conducting micropolar fluids without body forces, body couples and heat sources are given by:

$$D_1\vec{v}+\left(\lambda^f+\mu^f\right)\nabla\left(\nabla.\vec{v}\right)+K^f\left(\nabla\times\vec{\Psi}\right)-b\nabla T^f-c_0\nabla\phi^{*f}=0\,, \tag{4}$$

$$D_2\vec{\Psi}+\left(\alpha^f+\beta^f\right)\nabla\left(\nabla.\vec{\Psi}\right)+K^f\left(\nabla\times\vec{v}\right)=0\,, \tag{5}$$

$$K_1^* \nabla T^f - bT_0^f \left(\nabla . \vec{v}\right) = \rho^f a T_0^f \frac{\partial T^f}{\partial t}, \tag{6}$$

$$\rho^f \frac{\partial \phi^{*f}}{\partial t} = \nabla . \vec{v}, \tag{7}$$

where

$$D_1 = \left(\mu^f + K^f\right)\Delta - \rho^f \frac{\partial}{\partial t},\ D_2 = \gamma^f \Delta - I\frac{\partial}{\partial t} - 2K^f,\ \Delta g_i = g_{,ii} \tag{8}$$

and superscript f denotes physical quantities and material constants related to the fluid

The constitutive relations are

$$\begin{aligned} &t_{ij}^f = -p\delta_{ij} + \sigma_{ij}^f,\ p = bT^f + c_0\phi^{*f}, \\ &\sigma_{ij}^f = \lambda^f \gamma_{rr}\delta_{ij} + \left(\mu^f + K^f\right)\gamma_{ij} + \mu^f \gamma_{ji}\,, m_{ij}^f = \alpha^f \upsilon_{rr}\delta_{ij} + \beta^f \upsilon_{ji} + \gamma^f \upsilon_{ij}\,, \end{aligned} \tag{9}$$

where $\gamma_{ij} = v_{j,i} + \varepsilon_{jir}\Psi_r$, $\upsilon_{ij}=\Psi_{j,i}$ and symbols have their usual meaning as defined by Ciarletta [25].

3 FORMULATION OF THE PROBLEM

We consider a homogeneous, isotropic generalized thermoelastic half-space (medium M_1) in contact with heat conducting micropolar fluid half-space (medium M_2). The rectangular Cartesian co-ordinate system $O\,x_1x_2x_3$ having origin on the surface $x_3 = 0$ seperating the two media is taken. Let us take the x_1-axis along the interface between two half-spaces namely $M_1\,(0 < x_3 < \infty)$ and $M_2\,(-\infty < x_3 < 0)$ in such a way that x_3-axis is pointing vertically downward into the medium M_1. The geometry of the problem is shown in Fig. 1.

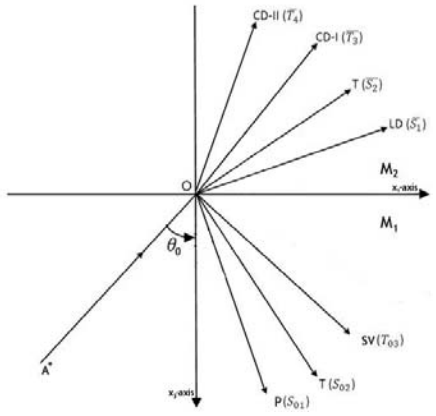

Fig.1
Geometry of the problem.

For two dimensional problem in x_1x_3-plane, we take the displacement vector $\vec{u}$, velocity vector $\vec{v}$ and microrotation velocity vector $\vec{\Psi}$ as:

$$\vec{u} = \left(u_1\left(x_1, x_3\right),\ 0,\ u_3\left(x_1, x_3\right)\right), \vec{v} = \left(\ v_1\left(x_1, x_3\right), 0\,, v_3(x_1, x_3)\right),\quad \vec{\Psi} = (0\,, \Psi_2(x_1, x_3), 0) \tag{10}$$

We take the following non dimensional quantities

$$x_i^{'} = \frac{\omega^* x_i}{c_1},\ u_i^{'} = \frac{\rho\omega^* c_1}{\nu T_0}u_i,\ v_i^{'} = \frac{\rho c_1}{\nu T_0}v_i,\ \psi_2^{'} = \frac{\rho c_1^{\,2}}{\omega^*\nu T_0}\psi_2,\ (t^{'},\tau_0^{'},\tau_1^{'}) = (\omega^* t,\ \omega^*\tau_0, \omega^*\tau_1),$$
$$(T^{'}, T^{f'}) = (\frac{T}{T_0}, \frac{T^f}{T_0}),\ (t_{ij}^{'}, t_{ij}^{f'}) = \frac{1}{\nu T_0}(t_{ij}, t_{ij}^f),\ m_{ij}^{f'} = \frac{\omega^*}{c_1\nu T_0}m_{ij}^f,\ \phi^{*f'} = \rho\phi^{*f} \tag{11}$$

where $\omega^* = \dfrac{\rho c^* c_1^2}{K^*}$, $\qquad c_1^2 = \dfrac{\lambda + 2\mu}{\rho}$

The expressions relating the displacement components u_1, u_3 and velocity component v_1, v_3 to the potential functions ϕ^s, ϕ^f and ψ^s, ψ^f in dimensionless form are taken as :

$$(u_1, v_1) = (\frac{\partial}{\partial x_1}(\phi^s, \phi^f) - \frac{\partial}{\partial x_3}(\psi^s, \psi^f)), \qquad (u_3, v_3) = (\frac{\partial}{\partial x_3}(\phi^s, \phi^f) + \frac{\partial}{\partial x_1}(\psi^s, \psi^f)), \tag{12}$$

4 BOUNDARY CONDITIONS

The boundary conditions at the interface $x_3 = 0$ are the continuity of components of normal stress, tangential stress, normal velocity, tangential velocity, thermodynamic temperature and normal component of heat flux and vanishing of tangential couple stress. Mathematically these can be written as :

$$t_{33} = t_{33}^f,\ \ t_{31} = t_{31}^f,\ \ \frac{\partial u_3}{\partial t} = v_3,\ \ \frac{\partial u_1}{\partial t} = v_1,\ \ T = T^f,\ \ \mathrm{K}^* \frac{\partial T}{\partial x_3} = K_1^* \frac{\partial T^f}{\partial x_3},\ \ m_{32}^f = 0 \tag{13}$$

5 REFRLECTION AND TRANSMISSION

We consider Longitudinal wave (P-wave), Thermal wave (T-wave) and Transverse wave (SV-wave) propagating through the medium M_1 which we designate as the region $x_3 > 0$ and incident at the plane $x_3 = 0$ with its direction of propagation with angle θ_0 normal to the surface. Corresponding to each incident wave, we get reflected P-wave, T-wave and SV-wave in medium M_1 and transmitted Longitudinal displacement wave (LD-wave), Thermal wave (T-wave), coupled transverse displacement and coupled transverse microrotational waves (CD-I wave and CD-II wave) in medium M_2 as shown in Fig. 1.

In order to solve the Eqs. (13)-(20), we assume the solutions of the system of the form:

$$\left\{\phi^s, T, \psi^s, \phi^f, \phi^{*f}, T^f, \psi^f, \Psi_2\right\} = \left\{\overline{\phi^s}, \overline{T}, \overline{\psi^s}, \overline{\phi^f}, \overline{\phi^{*f}}, \overline{T^f}, \overline{\psi^f}, \overline{\Psi_2}\right\} e^{\iota\left\{k\left(x_1 \sin\theta - x_3 \cos\theta\right) - \omega t\right\}} \tag{14}$$

where k is the wave number, ω is the angular frequency and $\overline{\phi^s}, \overline{T}, \overline{\psi^s}, \overline{\phi^f}, \overline{\phi^{*f}}, \overline{T^f}, \overline{\psi^f}, \overline{\Psi_2}$ are arbitrary constants.

In view of Eq. (14) and with the aid of (1), (2), (4)-(7) and (10)-(12), the appropriate potentials for medium M_1 and medium M_2 are taken as:

Medium M_1 :

$$\{\phi^s, T\} = \sum_{i=1}^{2}\{1, f_i\}[S_{0i} e^{\iota\left\{k_i\left(x_1 \sin\theta_{0i} - x_3 \cos\theta_{0i}\right) - \omega_i t\right\}} + P_i] \tag{15}$$

$$\psi^s = S_{03}e^{\iota\{k_3(x_1\sin\theta_{03}-x_3\cos\theta_{03})-\omega_3 t\}} + S_3 e^{\iota\{k_3(x_1\sin\theta_{03}+x_3\cos\theta_{03})-\omega_3 t\}} \tag{16}$$

where

$$f_i = \frac{\varepsilon_1\omega_i^2(\frac{\iota}{\omega_i}+\eta_0\tau_0)}{-\frac{1}{V_i^2}+(\frac{\iota}{\omega_i}+\tau_0)-\iota\varepsilon_1\omega_i(\frac{\iota}{\omega_i}+\eta_0\tau_0)(\frac{\iota}{\omega_i}+\tau_1)} \qquad \text{and} \qquad P_i = S_i e^{\iota\{k_i(x_1\sin\theta_i+x_3\cos\theta_i)-\omega_i t\}}$$

Medium M_2 :

$$\{\phi^f, T^f, \phi^{*f}\} = \sum_{i=1}^{2}\{1, \overline{f_i}, \overline{g_i}\}\overline{S_i}e^{\iota\{\overline{k_i}(x_1\sin\overline{\theta_i}-x_3\cos\overline{\theta_i})-\overline{\omega_i}t\}} \tag{17}$$

$$\{\psi^f, \Psi_2\} = \sum_{j=3}^{4}\{1, \overline{f_j}\}\overline{S_j}e^{\iota\{\overline{k_j}(x_1\sin\overline{\theta_j}-x_3\cos\overline{\theta_j})-\overline{\omega_j}t\}} \tag{18}$$

where

$$\overline{f_i} = \frac{-b_3 b_9}{b_1 b_9\frac{\iota}{\omega_i}+\iota\omega_i(1-\frac{\iota b_2 b_{11}}{\omega_i})(\frac{1}{\overline{V_i}^2}-b_{10}\frac{\iota}{\omega_i})}, \qquad \overline{f_j} = \frac{b_6(\frac{b_4}{\omega_j^2}+b_5\frac{\iota}{\omega_j})}{-\frac{1}{\overline{V_j}^2}-\frac{b_7}{\omega_j^2}+b_8\frac{\iota}{\omega_j}}, \qquad \overline{g_i} = \frac{-\iota b_{11}\omega_i}{\overline{V_i}^2}$$

and V_1, V_2 are the velocities of P-wave, T-wave in medium M_1 and these are roots of the Eq. (I-1) as given in Appendix I and $V_3 = \frac{1}{\sqrt{a_1}}$ is the velocity of SV-wave in medium M_1 . $\overline{V_1}, \overline{V_2}, \overline{V_3}, \overline{V_4}$ are the velocities of transmitted coupled LD-wave, T-wave, CD-I wave and CD-II wave in medium M_2 and these are roots of Eq. (I-2) and (I-3) as given in Appendix I.

S_{0i} , S_{03} are the amplitudes of incident (P-wave, T-wave) and SV-wave respectively. S_i and S_3 are the amplitudes of reflected (P-wave, T-wave) and SV-wave and $\overline{S_i}$, $\overline{S_j}$ are the amplitudes of transmitted longitudinal displacement wave, thermal wave and transverse wave coupled with microrotational wave respectively.

Eq. (17) represents the relation between (ϕ^f and T^f) ; (ϕ^f and ϕ^{f*}).

Following Singh and Tomar [23] , the extension of the Snell's law is given by:

$$\frac{\sin\theta_0}{V_0} = \frac{\sin\theta_1}{V_1} = \frac{\sin\theta_2}{V_2} = \frac{\sin\theta_3}{V_3} = \frac{\sin\overline{\theta_1}}{\overline{V_1}} = \frac{\sin\overline{\theta_2}}{\overline{V_2}} = \frac{\sin\overline{\theta_3}}{\overline{V_3}} = \frac{\sin\overline{\theta_4}}{\overline{V_4}} \tag{19}$$

where

$$k_1V_1 = k_2V_2 = k_3V_3 = \overline{k_1}\,\overline{V_1} = \overline{k_2}\,\overline{V_2} = \overline{k_3}\,\overline{V_3} = \overline{k_4}\,\overline{V_4} = \omega\,, \text{ at } x_3 = 0. \tag{20}$$

Making use of the values of $\phi^s, T, \psi^s, \phi^f, T^f, \phi^{*f}, \psi^f$ and Ψ_2 given by Eqs. (15)-(18) in the boundary conditions (13) and with the help of Eqs. (3), (9), (11), (12), (19) and (20), we obtain a system of seven non-homogeneous equations which can be written as :

$$\sum_{j=1}^{7} a_{ij}Z_j = Y_i\,;(i = 1, 2, 3, 4, 5, 6, 7) \tag{21}$$

where the values of a_{ij} are given in Appendix II

For incident P-wave:

$$A^* = S_{01}, S_{02} = S_{03} = 0, Y_1 = -a_{11}, Y_2 = a_{21}, Y_3 = a_{31} = 0, Y_4 = -a_{41}, Y_5 = a_{51}, Y_6 = -a_{61}, Y_7 = a_{71}$$

For incident T-wave:

$$A^* = S_{02}, S_{01} = S_{03} = 0, Y_1 = -a_{12}, Y_2 = a_{22}, Y_3 = a_{32} = 0, Y_4 = -a_{42}, Y_5 = a_{52}, Y_6 = -a_{62}, Y_7 = a_{72} = 0$$

For incident SV-wave:

$$A^* = S_{03}, S_{01} = S_{02} = 0, Y_1 = -a_{13}, Y_2 = -a_{23}, Y_3 = a_{33}, Y_4 = a_{43}, Y_5 = -a_{53}, Y_6 = a_{63} = 0, Y_7 = a_{73} = 0$$

and

$$Z_1 = \frac{S_1}{A^*}, \quad Z_2 = \frac{S_2}{A^*}, \quad Z_3 = \frac{S_3}{A^*}, \quad Z_4 = \frac{\overline{S_1}}{A^*}, \quad Z_5 = \frac{\overline{S_2}}{A^*}, \quad Z_6 = \frac{\overline{S_3}}{A^*}, \quad Z_7 = \frac{\overline{S_4}}{A^*} \tag{22}$$

where Z_1, Z_2, Z_3 are the amplitude ratios of reflected P-wave, T-wave and SV-wave in medium M_1 and Z_4, Z_5, Z_6, Z_7 are the amplitude ratios of transmitted LD-wave, T-wave and coupled CD-I, CD-II waves in medium M_2.

6 SPECIAL CASES

1. If $\eta_0 = 1, \tau_1 = 0$, in Eq. (21), then we obtain the corresponding amplitude ratios at an interface of thermoelastic solid half-space and heat conducting micropolar fluid half-space for L-S theory.
2. If $\eta_0 = 0, \tau_1 > 0$, in Eq. (21), then we obtain the corresponding amplitude ratios at an interface of thermoelastic solid half-space and heat conducting micropolar fluid half-space for G-L theory.
3. Neglecting the micropolar effect in medium M_2 i.e. let $K^f \to 0$, we obtain the amplitude ratios at the interface of heat conducting elastic solid and fluid media.

7 NUMERICAL RESULTS AND DISCUSSION

The following values of relevant parameters for both the half- spaces for numerical computations are taken.

Following Singh and Tomar [23], the values of micropolar constants for medium M_1 are taken as:

$$\lambda = 0.209730 \times 10^{10}\, Nm^{-2}, \ \mu = 0.91822 \times 10^{9}\, Nm^{-2}, \ \rho = 0.0034 \times 10^{3}\, Kgm^{-3},$$

and thermal Parameters are taken from Dhaliwal and Singh [16]:

$$\nu = 0.268 \times 10^{7}\, Nm^{-2}K^{-1}, \ c^* = 1.04 \times 10^{3}\, NmKg^{-1}K^{-1}, K^* = 1.7 \times 10^{2}\, Nsec^{-1}K^{-1},$$

$$T_0 = 0.298K, \quad \tau_0 = 0.613 \times 10^{-12}\, sec, \quad \tau_1 = 0.813 \times 10^{-12}\, sec, \quad \omega = 1$$

Following Singh and Tomar [24], the values of micropolar constants for medium M_2 are taken as:

$\lambda^f = 1.5\times10^8\, Nsecm^{-2}$, $\mu^f = 0.03\times10^8\, Nsecm^{-2}$, $K^f = 0.000223\times10^8\, Nsecm^{-2}$,
$\gamma^f = 0.0000222N\,\text{sec}$, $\rho^f = 0.8\times10^3\, Kgm^{-3}$, $I = 0.00400\times10^{-16}\, Nsec^2m^{-2}$

Thermal Parameters for the medium M_2 are taken as of comparable magnitude:

$T_0^f = 0.196K$, $K_1^* = 0.89\times10^2\, Nsec^{-1}K^{-1}$, $c_0 = 0.005\times10^{11}\, Nsec^2m^{-6}$, $a = 1.5\times10^5\, m^2sec^{-2}K^{-2}$
$b = 1.6\times10^5\, Nm^{-2}K^{-1}$

The values of amplitude ratios have been computed at different angles of incidence.

In Figs. 2-22, the variations of amplitude ratios at an interface of heat conducting elastic solid half-space and micropolar fluid half-space have been represented by solid line for L-S theory (LS1) and by small dashes line for G-L theory (GL1) respectively. Similarly, the variations of amplitude ratios at an interface of heat conducting elastic solid half-space and micropolar fluid half-space have been represented by medium dashes line for L-S theory (LS2) and by large dashes line for G-L theory (GL2) respectively.

7.1 P-Wave Incident

Variations of amplitude ratios $|Z_i|; 1 \le i \le 7$ with the angle of incidence θ_0 , for incident P- wave are shown in Figs. 2 through 8.

Fig. 2 depicts that the values of $|Z_1|$ for LS1 and GL1 decrease in the range $0^0 < \theta_0 < 65^0$ and then increase in the further range. It is noticed that the values of $|Z_1|$ for LS1 remain more than the values for LG1 in the whole range. The values of $|Z_1|$ for LS2 and GL2 increase and the values for LS1 remain less than the values for GL2 in the whole domain.

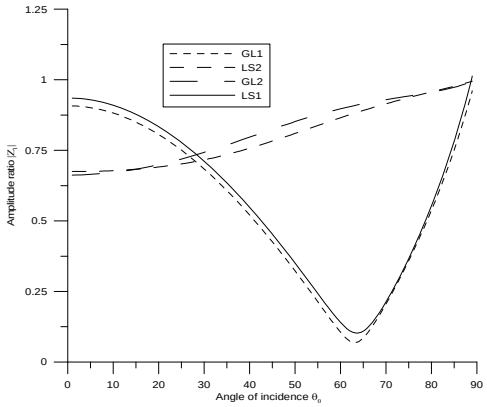

Fig.2
Variation of $|Z_1|$ with angle of incidence (P-wave).

Fig. 3 depicts that the values of $|Z_2|$ for LS1 and GL1 oscillate as θ_0 increases and the values for LS2 and GL2 decrease in the whole range, but the values for GL2 remain more than the values for LS2 in the whole range. The values for LS1 are greater than the values for GL1 in the whole range, except for some finite range, where the behavior is reversed.

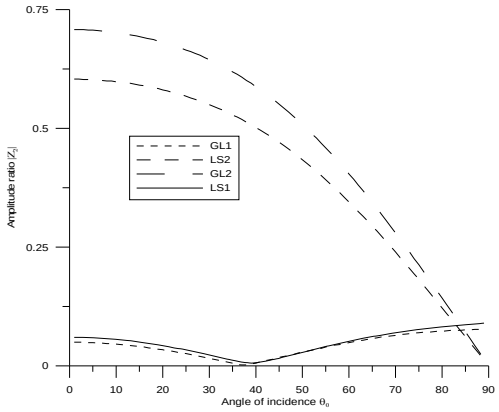

Fig.3
Variation of $|Z_2|$ with angle of incidence (P-wave).

Fig. 4 shows that the values of $|Z_3|$ for LS2 and GL2 increase in the interval $0^0 < \theta_0 < 52^0$ and then decrease with increase in θ_0. It is observed, that the values for LS1 in comparison with LS2 and GL1 in comparison with GL2 remain more in the whole domain that reveals the effect of micropolarity.

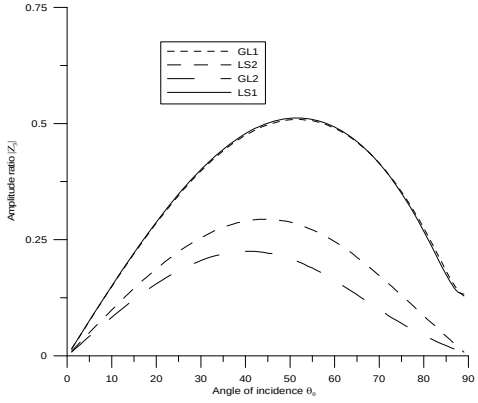

Fig.4
Variation of $|Z_3|$ with angle of incidence (P-wave).

Fig. 5 depicts that the values of $|Z_4|$ for GL1 are greater than the values for LS1 in the whole range, except near the grazing incidence, where the behavior is reversed. The values for LS2 and GL2 decrease in the whole range, but the values for GL2 remain more than the values for LS2 in the whole range. The values for $|Z_4|$ for LS1 and GL1 are magnified by multiplying its original value by 10^2 and LS2, GL2 by 10.

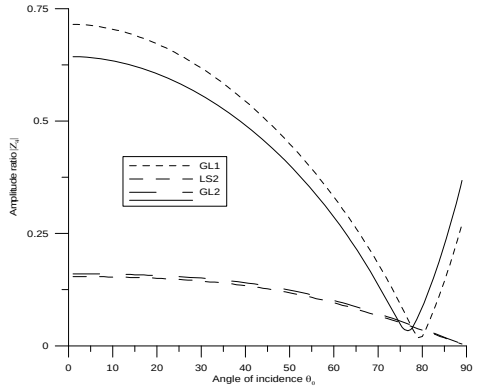

Fig.5
Variation of $|Z_4|$ with angle of incidence (P-wave).

Fig. 6 depicts that the values of $|Z_5|$ for LS1, GL1 decrease in the range $0^0 < \theta_0 < 65^0$ and $0^0 < \theta_0 < 50^0$ respectively and in the remaining range, the behavior is reversed and the values for LS1 are greater than the values

for GL1 in the whole domain. The values for $|Z_5|$ for LS1 and GL1 are magnified by multiplying its original value by 10^2 and LS2, GL2 by 10.

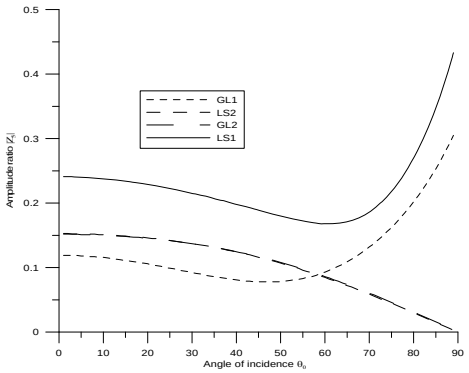

Fig.6
Variation of $|Z_5|$ with angle of incidence (P-wave).

Fig. 7 shows that the behavior of $|Z_6|$ for LS1 in comparison with GL1 and LS2 in comparison with GL2 is similar in the whole range with difference in magnitude. The values of amplitude ratio for GL1 in comparison with LS1 and LS2 in comparison with GL2 are greater in the whole range. The values of $|Z_6|$ for LS1, GL1, LS2 and GL2 are magnified by multiplying its original value by 10^2.

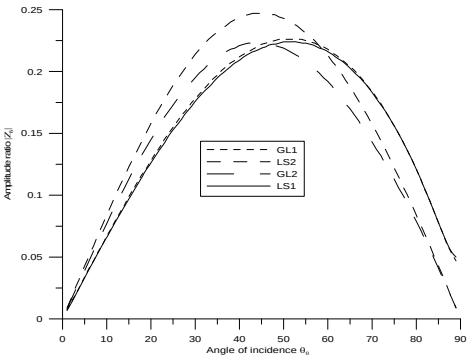

Fig.7
Variation of $|Z_6|$ with angle of incidence (P-wave).

Fig. 8 depicts that the values of $|Z_7|$ for LS1 and GL1 increase in the range $0^0 < \theta_0 < 52^0$ and decrease in the further range. The values of amplitude ratio for GL1 remain more than the values for LS1 in the whole domain. The values for $|Z_7|$ for LS1 and GL1 are magnified by multiplying its original value by 10^6.

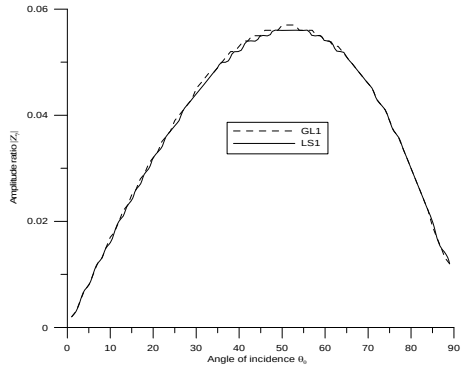

Fig.8
Variation of $|Z_7|$ with angle of incidence (P-wave).

7.2 T-Wave Incident

Variations of amplitude ratios $|Z_i|; 1 \le i \le 7,$ with the angle of incidence θ_0, for incident T-wave are shown in Figs. 9-15.

Fig. 9 depicts that the behavior of variation of $|Z_1|$ for LS1, GL1, LS2 and GL2 is oscillatory as θ_0 increases and the values of amplitude ratio for LS1 in comparison with GL1, except near the normal incidence and LS2 in comparison with GL2 remain more in the whole range.

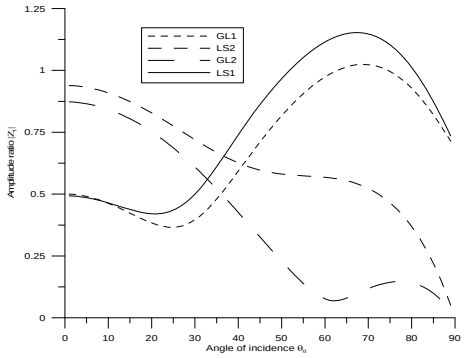

Fig.9
Variation of $|Z_1|$ with angle of incidence (T-wave) .

Fig. 10 depicts that the behavior of variation of $|Z_2|$ for LS1 in comparison with GL1 and LS2 in comparison with GL2 is similar in the whole range with difference in magnitude. The values of amplitude ratio for GL1 remain more than the values for LS1 in range $0^0 < \theta_0 < 56^0$ and in the further range, the behavior is reversed and the values for GL2 remain more than the values for LS2 in the range $0^0 < \theta_0 < 66^0$ and reversed behavior is observed in the further range.

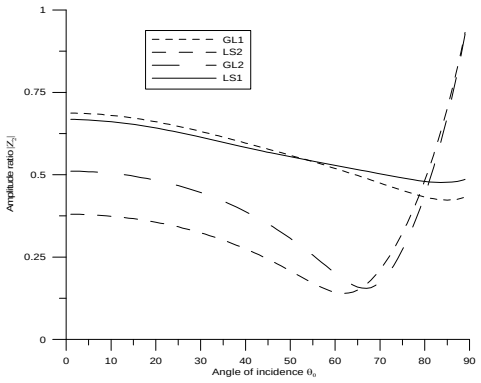

Fig.10
Variation of $|Z_2|$ with angle of incidence (T-wave).

It is depicted from fig. 11 that the values of $|Z_3|$ for LS1, GL1, LS2 and GL2 first increase and then decrease with increase in θ_0 and the values of amplitude ratio for LS2 remain more than the values of amplitude ratio for GL2 in the whole range and the maximum value is attained by LS1 within the interval $60^0 < \theta_0 < 70^0$. The values of amplitude ratio for LS1 in comparison with LS2 and GL1 in comparison with GL2 remain more in the whole range due to the effect of micropolarity.

Fig. 12 depicts that the values of $|Z_4|$ for LS2 and GL2 decrease with increase in θ_0, but the values for LS1 and GL1 oscillate. The values of amplitude ratio for LS1 in comparison with GL1 and LS2 in comparison with GL2 remain more in the whole range. The values for $|Z_4|$ for LS1 and GL1 are magnified by multiplying its original value by 10.

Fig. 13 depicts that the values of $|Z_5|$ for is similar as that for LS1, GL1, LS2 and GL2 decrease in the whole range with slight increase in the values for GL1, LS1 near the grazing incidence. The values for $|Z_5|$ for LS1, GL1, LS2 and GL2 are magnified by multiplying its original value by 10.

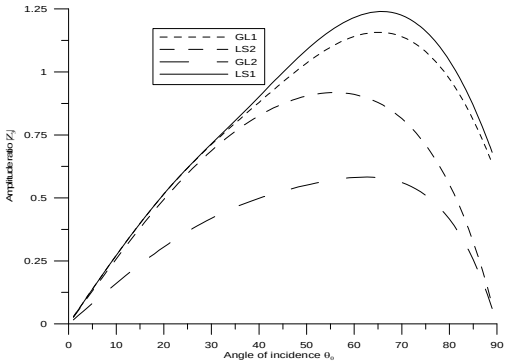

Fig.11
Variation of $|Z_3|$ with angle of incidence (T-wave).

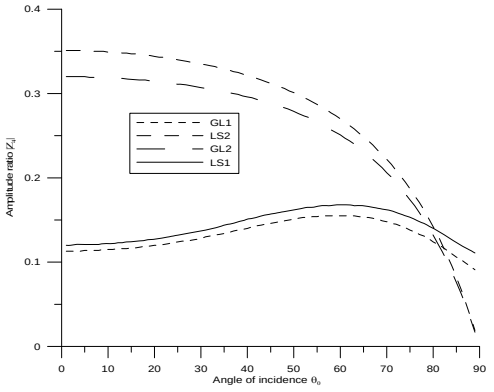

Fig.12
Variation of $|Z_4|$ with angle of incidence (T-wave).

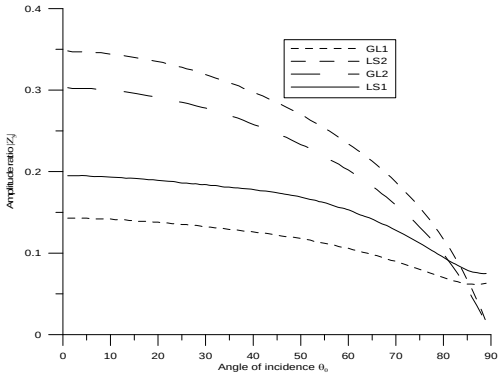

Fig.13
Variation of $|Z_5|$ with angle of incidence (T-wave).

Fig. 14 depicts that the values of $|Z_6|$ for LS1 and GL1 increase with increase in θ_0, except near the grazing incidence, where the behavior is reversed. The values of amplitude ratio for LS2 and GL2, first increase and then decrease with increase in θ_0 with slight difference in their magnitude. The values for LS1 remain more than the values for GL1 in the whole range, except near the grazing incidence, where the behavior is reversed. The values for $|Z_6|$ for LS1, GL1 are magnified by multiplying its original value by 10 and LS2, GL2 are magnified by multiplying its original value by 10^2.

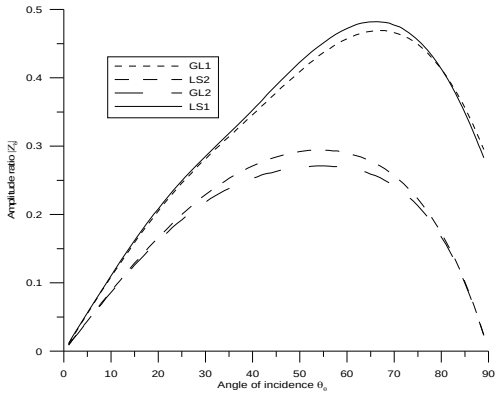

Fig.14
Variation of $|Z_6|$ with angle of incidence (T-wave).

Fig. 15 depicts the values of $|Z_7|$ for LS1 remain more than the values for GL1 in the whole range, except near the grazing incidence, where the behavior is reversed. The values for $|Z_7|$ for LS1 and GL1 are magnified by multiplying its original value by 10^6.

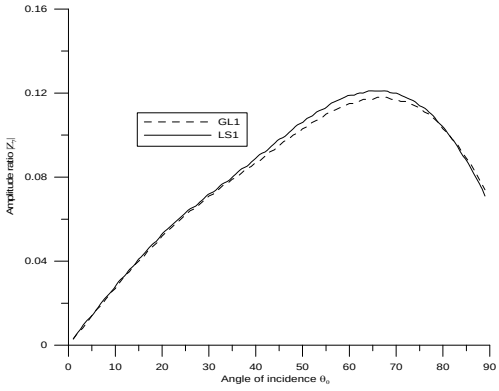

Fig.15
Variation of $|Z_7|$ with angle of incidence for (T-wave) .

7.3 SV-Wave Incident

Variations of amplitude ratios $|Z_i|; 1 \le i \le 7$, with the angle of incidence θ_0, for incident SV-wave are shown in Figs. 16-22.

Fig. 16 depicts that the behavior of $|Z_1|$ for LS1, GL1, LS2 and GL2 is oscillatory as θ_0 increases. The values for LS1 and GL1 attain peak value at $\theta_0 = 45^0$. The values for GL2 and LS2 attain minima at $\theta_0 = 45^0$.

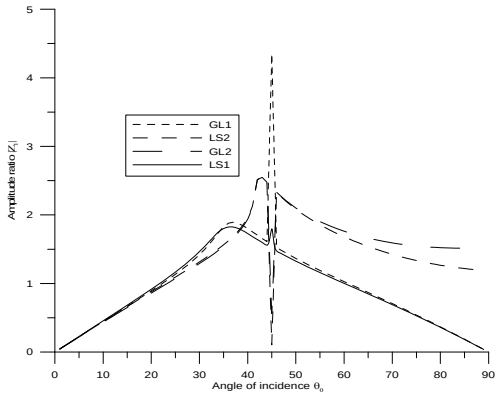

Fig.16
Variation of $|Z_1|$ with angle of incidence (SV- wave).

Fig. 17 shows that the behavior of variation of $|Z_2|$ for LS1 in comparison with GL1 and LS2 in comparison with GL2 is similar in the whole range with difference in magnitude. The values of amplitude ratio for GL2 remain more than the values for LS2 in the whole range.

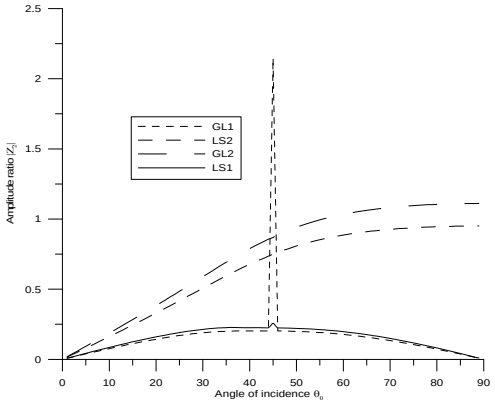

Fig.17
Variation of $|Z_2|$ with angle of incidence (SV- wave).

Fig. 18 depicts that the values of $|Z_3|$ for LS1, GL1, LS2 and GL2 oscillate with increase in θ_0. The behavior of oscillation of LS1 in comparison with GL1 and LS2 in comparison with GL2 is similar with difference in their magnitude values.

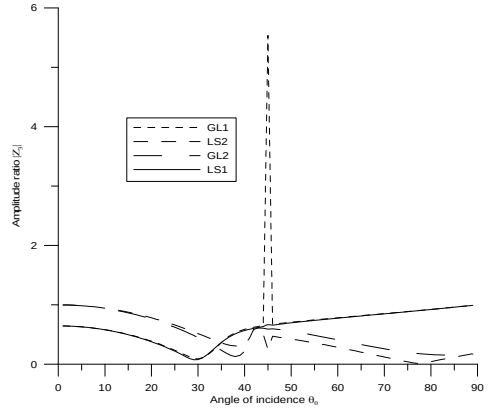

Fig.18
Variation of $|Z_3|$ with angle of incidence (SV-Wave).

Fig. 19 shows that the values of $|Z_4|$ for LS1 remain more than the values for LS1 in the whole domain. The values for LS2 and GL2 increase with θ_0 with oscillation within the range $42^0 < \theta_0 < 47^0$. The values for $|Z_4|$ for LS1 and GL1 ,LS1 and GL2 are magnified by multiplying its original value by 10.

Fig. 20 depicts that the values of $|Z_5|$ for GL1 attain peak value at $\theta_0 = 45^0$. The values for LS2 and GL2 oscillate with slight difference in their magnitudes. The values for $|Z_5|$ for LS1, GL1, LS2 and GL2 are magnified by multiplying its original value by 10.

Fig. 21 depicts that the values of $|Z_6|$ for LS1 and GL1 oscillate in the whole range with difference in magnitude. The values for GL2 remain more than the values for LS2 in the whole range .The values for $|Z_6|$ for LS1, GL1, LS2 and GL2 are magnified by multiplying its original value by 10^2.

Fig. 22 depicts that the values of $|Z_7|$ for LS1 and GL1 attain maximum value at the normal incidence. The magnitude of amplitude ratios for LS1 and GL1 is very small. The values for $|Z_7|$ for LS1 and GL1 are magnified by multiplying its original value by 10^6.

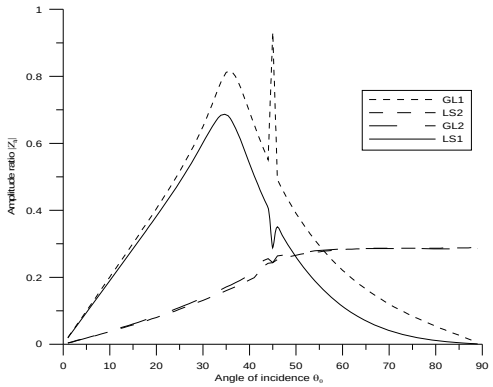

Fig.19
Variation of $|Z_4|$ with angle of incidence (SV- wave).

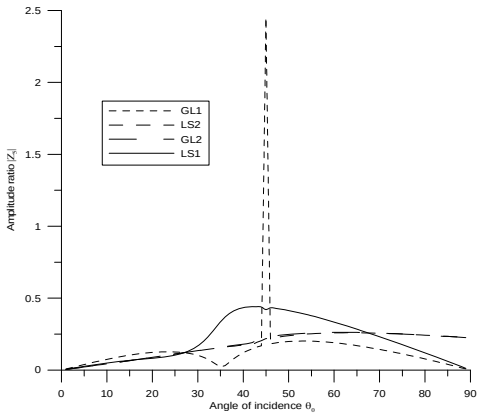

Fig.20
Variation of $|Z_5|$ with angle of incidence (SV- Wave).

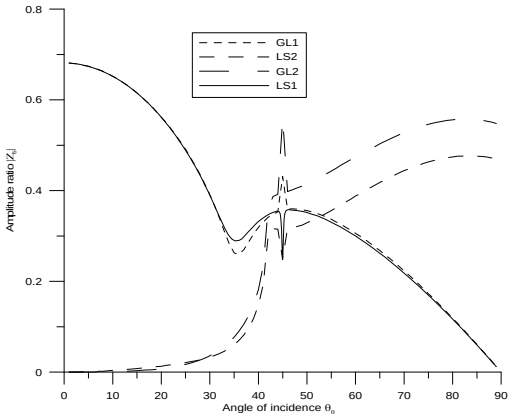

Fig.21
Variation of $|Z_6|$ with angle of incidence (SV-Wave).

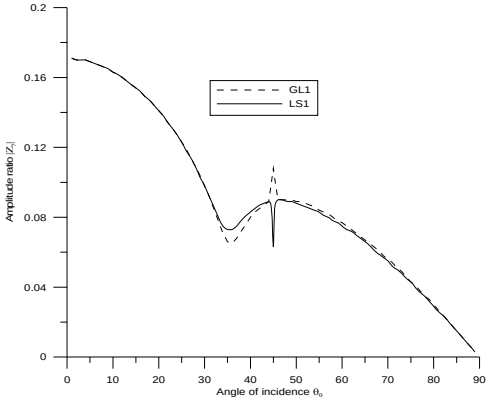

Fig.22
Variation of $|Z_7|$ with angle of incidence (SV-wave).

8 CONCLUSION

Detailed numerical calculations have been presented for the cases of incidence of P-wave, T-wave and SV-wave at the plane surface of model considered. Appreciable micropolarity and thermal relaxation effects have been observed on amplitude ratios, for incidence of various plane waves (P-wave ,T-wave and SV-wave). It is observed that the values of amplitude ratios are more oscillatory in case of incidence of SV-wave as compared to the values of amplitude ratios for incidence of P-wave and T-wave. The values of $|Z_i|; i = 1, 2, 4$ for GL2 remain more than the values for LS2 when P-wave is incident. It is noticed that the values of amplitude ratios $|Z_i|; i = 3 \le i \le 5$ for LS1 (with one relaxation time) are greater than the values for GL1 (with two relaxation times), when T-wave is incident. The values of amplitude ratios of reflected SV-wave and reflected CD-I wave for LS1 in comparison with LS2 and GL1 in comparison with GL2 are greater (when T-wave is incident) that reveals the effect of micropolarity.

Appendix I

$$V^4 + DV^2 + E = 0\,, \tag{I-1}$$

$$V^4 + D_2V^2 + E_2 = 0\,, \tag{I-2}$$

$$V^4 + D_3V^2 + E_3 = 0\,, \tag{I-3}$$

where

$$D_1 = -\frac{\left[1+(1-\iota\tau_1\omega)\varepsilon_1\left(\frac{\iota}{\omega}+\eta_0\tau_0\right)\right]}{\tau_{00}} - 1, \quad E_1 = \frac{1}{\tau_{00}}, \quad D_2 = \frac{l\omega}{b_3}\left(1-\frac{\iota b_2 b_{11}}{\omega}\right) + \frac{\iota\omega}{b_{10}}\left(1+\frac{\iota b_1 b_9}{\omega b_3}\right),$$

$$E_2 = \frac{\omega^2}{b_3 b_{10}}\left(-1+\frac{\iota b_2 b_{11}}{\omega}\right), \quad D_3 = \frac{\iota\omega}{b_5} + \iota\omega\frac{\left(1-\frac{\iota b_4 b_6}{\omega b_5}\right)}{\left(b_8+\frac{\iota}{\omega}b_7\right)}, \quad E_3 = -\frac{\omega^2}{\left(b_8+\frac{\iota}{\omega}b_7\right)b_5}$$

$$a_1 = \frac{\rho c_1^2}{\mu}, \ \varepsilon_1 = \frac{\nu^2 T_0}{K^*\omega^*\rho}, \ b_1 = \frac{b\rho c_1^2}{(\lambda^f + 2\mu^f + K^f)\omega^*\nu}, \ b_2 = \frac{c_0 c_1^2}{(\lambda^f + 2\mu^f + K^f)\omega^*\nu T_0},$$

$$b_3 = \frac{\rho^f c_1^2}{(\lambda^f + 2\mu^f + K^f)\omega^*}, \ b_4 = \frac{K^f}{\mu^f + K^f}, \ b_5 = \frac{\rho^f c_1^2}{\left(\mu^f + K^f\right)\omega^*}, \ b_6 = \frac{K^f c_1^2}{\gamma^f \omega^{*2}}, \quad \tau_{00} = \frac{1}{\frac{\iota}{\omega}+\tau_0}$$

$$b_7 = 2b_6\,, \quad b_8 = \frac{\mathrm{I}c_1^2}{\gamma^f\omega^*}\,, \quad b_9 = \frac{b\nu T_0^f}{K_1^*\rho\omega^*}\,, \quad b_{10} = \frac{\rho^f a T_0^f c_1^2}{K_1^*\omega^*}, \quad b_{11} = \frac{\nu T_0}{\rho^f c_1^2}, \quad V = \frac{\omega}{k}$$

and $\nabla = \frac{\partial^2}{\partial x_1^{\,2}} + \frac{\partial^2}{\partial x_3^{\,2}}$ is the Laplacian operator

Appendix II

$$a_{1i} = \left(d_1 + d_2 (1 - \frac{V_i^2}{V_0^2} \sin^2 \theta_0 \,) \right) + \left(\frac{V_1^2}{\omega^2} - \tau_1 \iota \frac{V_1^2}{\omega} \right) f_i \,, \qquad a_{13} = d_2 \frac{V_1^2}{V_3 V_0} \sin\theta_0 \sqrt{1 - \frac{V_3^2}{V_0^2} \sin^2 \theta_0} \,,$$

$$a_{1j} = -\left[\left(d_2^f + d_3^f (1 - \frac{\overline{V_i^2}}{V_0^2} \sin^2 \theta_0 \,) \right) \frac{V_1^2}{\overline{V_i^2}} + (\overline{f_i} d_1^{ff} + d_1^f \overline{g_i}) \frac{V_1^2}{\omega^2} \right],$$

$$a_{1k} = d_3^f \frac{V_1^2}{\overline{V_{j-1}^2} V_0} \sin\theta_0 \sqrt{1 - \frac{\overline{V_{j-1}^2}}{V_0^2} \sin^2 \theta_0} \,, \qquad a_{2i} = -2 d_3 \frac{V_i}{V_0} \sin\theta_0 \sqrt{1 - \frac{V_i^2}{V_0^2} \sin^2 \theta_0} \,,$$

$$a_{23} = d_3 \frac{V_1^2}{V_3^2} (1 - 2 \frac{V_3^2}{V_0^2} \sin^2 \theta_0 \,), \quad a_{2j} = -\left(2 d_4^f + d_5^f \right) \frac{V_1^2}{\overline{V_i} V_0} \sin\theta_0 \sqrt{1 - \frac{\overline{V_i^2}}{V_0^2} \sin^2 \theta_0} \,,$$

$$a_{2k} = -\left[d_4^f \frac{V_1^2}{\overline{V_{j-1}^2}} \left(1 - 2 \frac{\overline{V_{j-1}^2}}{V_0^2} \sin^2 \theta_0 \right) + d_5^f \left(\frac{V_1^2}{\overline{V_{j-1}^2}} \left(\sqrt{1 - \frac{\overline{V_{j-1}^2}}{V_0^2} \sin^2 \theta_0} \right) - \frac{V_1^2}{\omega^2} \overline{f_{j-1}} \right) \right],$$

$$a_{3i} = a_{33} = a_{3j} = 0 \,, \quad a_{3k} = \iota \frac{V_1}{\overline{V_{j-1}}} \sqrt{1 - \frac{\overline{V_{j-1}^2}}{V_0^2} \sin^2 \theta_0} \; f_{j-1} \,, \quad a_{4i} = \omega \frac{V_1}{V_0} \sin\theta_0 , \qquad \text{(II-1)}$$

$$a_{43} = -\omega \frac{V_1}{V_3} \sqrt{1 - \frac{V_3^2}{V_0^2} \sin^2 \theta_0} \,, \; a_{4j} = -\iota \frac{V_1}{\overline{V_i}} \sin\theta_0 , \qquad a_{4k} = -\iota \frac{V_1}{\overline{V_{j-1}}} \sqrt{1 - \frac{\overline{V_{j-1}^2}}{V_0^2} \sin^2 \theta_0} \,,$$

$$a_{5i} = \omega \sqrt{1 - \frac{V_i^2}{V_0^2}} \sin^2 \theta_0 \,, \quad a_{53} = \omega \frac{V_1}{V_0} \sin\theta_0 \;, \; a_{5j} = \iota \frac{V_1}{\overline{V_i}} \sqrt{1 - \frac{\overline{V_i^2}}{V_0^2} \sin^2 \theta_0} \,, \qquad a_{5k} = -\iota \frac{V_1}{V_0} \sin\theta_0 ,$$

$$a_{6i} = f_i \,, \; a_{63} = 0 \,, \; a_{6j} = -\overline{f_i} \,, \; a_{6k} = 0, \qquad a_{7i} = \iota \sqrt{1 - \frac{V_i^2}{V_0^2} \sin^2 \theta_0} \; f_i \,, \; a_{73} = 0 \,,$$

$$a_{7j} = \iota p_1 \frac{V_1}{\omega} \sqrt{1 - \frac{\overline{V_i^2}}{V_0^2} \sin^2 \theta_0} \; \overline{f_i} \,, \qquad a_{7k} = 0 \qquad\qquad (i = 1,\ 2, j = 4,5,\ \ k = 6,7)$$

where

$$d_1 = \frac{\lambda}{\rho c_1^2} \,, \quad d_2 = \frac{2\mu}{\rho c_1^2} \,, \quad d_4 = \frac{d_2}{2} \,, \quad d_1^{ff} = \frac{b}{\nu} \,, \quad d_1^f = \frac{c_0}{\rho \nu T_0} \,, \quad d_2^f = \frac{\lambda^f \omega^*}{\rho c_1^2} ,$$

$$d_3^f = \frac{(2\mu^f + K^f)\omega^*}{\rho c_1^2} , \qquad d_4^f = \frac{\mu^f \omega^*}{\rho c_1^2} , \qquad d_5^f = \frac{K^f \omega^*}{\rho c_1^2} , \qquad p_2 = \frac{K_1^*}{K^*}$$

REFERENCES

[1] Eringen A.C., 1964, Simple microfluids, *International Journal of Engineering Science* **2**: 205-217.

[2] Eringen A.C., 1966 a, Theory of microfluids, *Journal of Applied Mathematics and Mechanics* **16**: 1-18.

[3] Ariman T., Sylvester N.D., Turk M.A., 1973, Microcontinuum fluid mechanics-a review, *International Journal of Engineering Science* **11**: 905-930.

[4] Ariman T., Sylvester N.D., Turk M.A., 1974, Review article applications of microcontinuum fluid mechanics, *International Journal of Engineering Science* **12**: 273-293.
[5] Riha P., 1975, On the theory of heat-conducting micropolar fluid with microtemperature, *Acta Mechanica* **23**: 1-8.
[6] Eringen A.C., Kafadar C.B.,1976, *Polar Field Theories, In Continuum Physics* ,Edited by A.C. Eringen, Vol. IV. Academic Press, New York.
[7] Brulin O., 1982, *Linear Micropolar Media, In Mechanics of Micropolar Media* ,Edited by O. Brulin and R.K.T. HSIEH, World Scientific, Singapore.
[8] Gorla R.S.R.,1989, Combined forced and free convection in the boundary layer flow of a micropolar fluid on a continuous moving vertical cylinder, *International Journal of Engineering Science* **27**: 77-86.
[9] Eringen A.C., 1990, Theory of Microstretch and Bubbly Liquid, *International Journal of Engineering Science* **28**: 133-143.
[10] Aydemir N.U., Venart J.E.S., 1990, Flow of a thermomicropolar fluid with stretch, *International Journal of Engineering Science* **28**: 1211-1222.
[11] Hsia S.Y., Cheng J.W., 2006, Longitudinal plane waves propagation in elastic micropolar porous media, *Japanese Journal of Applied Physics* **45**: 1743-1748.
[12] Hsia S.Y., Chiu S.M., Su C.C., Chen T.H., 2007, Propagation of transverse waves in elastic micropolar porous semispaces, *Japanese Journal of Applied Physics* **46**: 7399-7405.
[13] Biot M., 1956, Thermoelasticity and Irreversible Thermodynamics, *Journal of Applied Physics* **27**: 240-253.
[14] Lord H., Shulman Y., 1967, A generalized dynamical theory of thermoelasticity, *Journal of the Mechanics and Physics of Solids* **15**: 299-309.
[15] Green A.E., Lindsay K.A., 1972, Thermoelasticity, *Journal of Elasticity* **2**: 1-7.
[16] Dhaliwal R.S., Singh A., 1980, *Dynamic Coupled Thermoelasticity*, Hindustan Publication Corporation, New Delhi, India.
[17] Ignaczak J., Starzewski M.O., 2010, *Thermoelasticity with Finite Wave Speeds*, Oxford Science Publisher.
[18] Tomar S.K., Gogna M.L., 1992, Reflection and refraction of a longitudinal microrotational wave at an interface between two micropolar elastic solids in welded contact, *International Journal of Engineering Science* **30**: 1637-1646.
[19] Tomar S.K., Gogna M.L., 1995 a, Reflection and refraction of a longitudinal displacement wave at an interface between two micropolar elastic solids in welded contact, *Journal of the Acoustical Society of America* **97**: 827-830.
[20] Tomar S.K., Gogna M.L., 1995 b, Reflection and refraction of a coupled transverse and microrotational waves at an interface between two different micropolar elastic solids in welded contact, *International Journal of Engineering Science* **30**: 485-496.
[21] Kumar R., Sharma N., Ram P., 2008 a, Reflection and transmission of micropolar elastic waves at an imperfect boundary, *Multidiscipline Modelling in Materials and Structures (MMMS)* **4**: 15-36.
[22] Kumar R., Sharma N., Ram P., 2008 b, Interfacial imperfection on reflection and transmission of plane waves in anisotropic micropolar media, *Theoretical and Applied Fracture Mechanics* **49**: 305-312.
[23] Singh D., Tomar S. K., 2008, Longitudinal waves at a micropolar fluid/solid interface, *International Journal of Solids And Structures* **45**: 225-244.
[24] Ciarletta M., 2001, Spatial decay estimates for heat conducting micropolar fluids, *International Journal of Engineering Science* **39**: 655-668.